Hemisynthetic alkaloids derived from trilobine are antimalarials with sustained activity in multidrug-resistant Plasmodium falciparum

Flore Nardella, Irina Dobrescu, Haitham Hassan, Fabien Rodrigues, Sabine Thiberge, Liliana Mancio-Silva, Ambre Tafit, Corinne Jallet, Véronique Cadet-Daniel, Stéphane Goussin, et al.

iScience

CellPress
OPEN ACCESS

Article

Hemisynthetic alkaloids derived from trilobine are antimalarials with sustained activity in multidrug-resistant *Plasmodium falciparum*

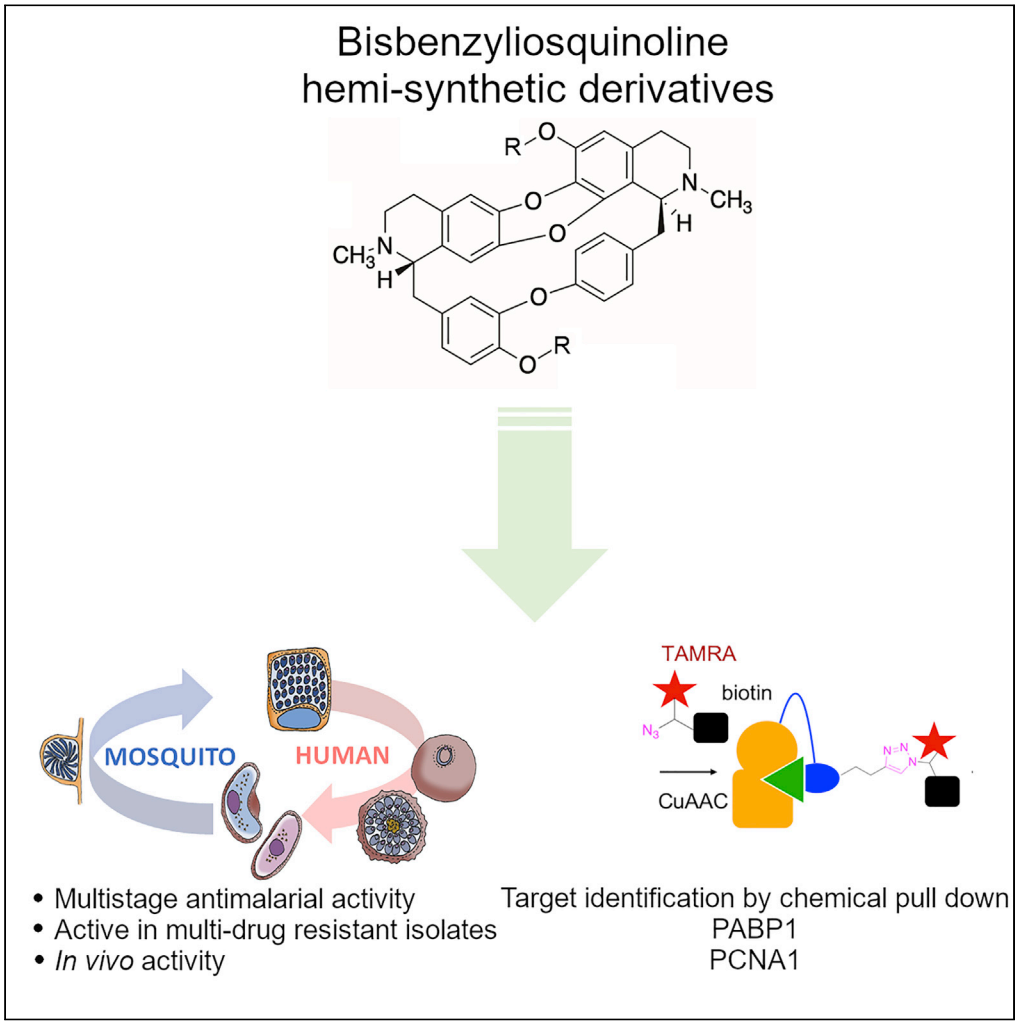

Flore Nardella, Irina Dobrescu, Haitham Hassan, ..., Artur Scherf, Ludovic Halby, Paola B. Arimondo

artur.scherf@pasteur.fr (A.S.)
paola.arimondo@cnrs.fr (P.B.A.)

Highlights

First hemisynthetic trilobine derivatives for malaria treatment

Compounds active in multi-drug resistant isolates of Cambodia

Target multiple malaria life cycle stages

Chemical pull-down enriched proteins involved in translation and DNA replication

Nardella et al., iScience *26*, 105940
February 17, 2023
https://doi.org/10.1016/j.isci.2023.105940

iScience

CellPress
OPEN ACCESS

Article

Hemisynthetic alkaloids derived from trilobine are antimalarials with sustained activity in multidrug-resistant *Plasmodium falciparum*

Flore Nardella,[1,8] Irina Dobrescu,[1,8] Haitham Hassan,[2,8] Fabien Rodrigues,[2] Sabine Thiberge,[1,3] Liliana Mancio-Silva,[1] Ambre Tafit,[2] Corinne Jallet,[2] Véronique Cadet-Daniel,[2] Stéphane Goussin,[3] Audrey Lorthiois,[3] Yoann Menon,[4] Nicolas Molinier,[4] Dany Pechalrieu,[4] Christophe Long,[4] François Sautel,[4] Mariette Matondo,[5] Magalie Duchateau,[5] Guillaume Médard,[6] Benoit Witkowski,[7] Artur Scherf,[1,*] Ludovic Halby,[2] and Paola B. Arimondo[2,4,9,*]

SUMMARY

Malaria eradication requires the development of new drugs to combat drug-resistant parasites. We identified bisbenzylisoquinoline alkaloids isolated from *Cocculus hirsutus* that are active against *Plasmodium falciparum* blood stages. Synthesis of a library of 94 hemi-synthetic derivatives allowed to identify compound 84 that kills multi-drug resistant clinical isolates in the nanomolar range (median IC_{50} ranging from 35 to 88 nM). Chemical optimization led to compound 125 with significantly improved preclinical properties. 125 delays the onset of parasitemia in *Plasmodium berghei* infected mice and inhibits *P. falciparum* transmission stages *in vitro* (culture assays), and *in vivo* using membrane feeding assay in the *Anopheles stephensi* vector. Compound 125 also impairs *P. falciparum* development in sporozoite-infected hepatocytes, in the low micromolar range. Finally, by chemical pull-down strategy, we characterized the parasite interactome with trilobine derivatives, identifying protein partners belonging to metabolic pathways that are not targeted by the actual antimalarial drugs or implicated in drug-resistance mechanisms.

INTRODUCTION

Malaria, a vector-borne disease, continues to cause morbidity and mortality with more than 247 million cases and 619,000 annual deaths according to the World Health Organization (WHO).[1] This disease is caused by an apicomplexan protozoan parasite belonging to the genus *Plasmodium*. Among the five *Plasmodium spp* that infect humans, *Plasmodium falciparum* is, by far, responsible for the most severe disease and greatest number of deaths.

P. falciparum has a complex life cycle: the parasite is transmitted to humans by a mosquito bite that inoculates sporozoites. Sporozoites rapidly reach the liver where they replicate exponentially in a hepatocyte for approximately one week before the cells burst and release merozoites into the bloodstream. The merozoites invade red blood cells (RBC) and evolve in a 48h cycle of asexual replication through three stages called ring, trophozoite, and schizont, that will ultimately release new merozoites. Some parasites invading RBC differentiate into gametocytes, that will evolve in five stages. Through a blood meal, female Anopheles mosquitoes uptake parasites, and the mature stage V gametocytes will differentiate into gametes and fuse to form a zygote. The zygote differentiates into a motile ookinete that crosses the mosquito midgut and encysts in the midgut wall (oocyst). Exponential replication occurs again in the oocyst leading to sporozoites. Rupture of the oocyst releases the sporozoites that reach the salivary glands, where they can lead to a new infection of the human host. Symptoms appear during the exponential asexual replication in RBC. A malaria episode is characterized by fever, headache, and chills. If untreated, malaria can rapidly evolve into a life-threatening state with multivisceral failure and coma.

Treatment relies on artemisinin derivatives used alone (severe malaria) or in combination (uncomplicated malaria) with chloroquine derivatives (amodiaquine, piperaquine, pyronaridine-targeting heme

[1]Biology of Host-Parasite Interaction, Department of Parasites and Insect Vectors, Institut Pasteur, Université de Paris-Cité, CNRS EMR 9195, INSERM Unit U1201, 25-28 Rue du Dr Roux, 75015 Paris, France

[2]Epigenetic Chemical Biology, Department of Structural Biology and Chemistry, Institut Pasteur, Université de Paris-Cité, UMR n°3523, CNRS, 28 Rue du Dr Roux, 75015 Paris, France

[3]Center for Production and Infection of Anopheles (CEPIA), Center for Animal Resources and Research, Institut Pasteur, 75015 Paris, France

[4]USR CNRS-Pierre Fabre No. 3388 ETaC, Centre de Recherche et Développement Pierre Fabre, 3 Avenue Hubert Curien, 31035 Toulouse Cedex 01, France

[5]Proteomics Platform, Mass Spectrometry for Biology Unit, Institut Pasteur, Université de Paris-Cité, CNRS USR 2000, 28 rue du Dr Roux, 75015 Paris, France

[6]Chair of Proteomics and Bioanalytics, TUM School of Life Sciences, 85354 Freising, Germany

[7]Malaria Molecular Epidemiology Unit, Pasteur Institute in Cambodia, Phnom Penh 12201, Cambodia

[8]These authors contributed equally

[9]Lead contact

*Correspondence: artur.scherf@pasteur.fr (A.S.), paola.arimondo@cnrs.fr (P.B.A.)

https://doi.org/10.1016/j.isci.2023.105940

crystallization), amino-alcohols (mefloquine, lumefantrine-targeting 80S ribosome[2]) or antifolates (sulfadoxine, pyrimetamine-targeting *Plasmodium* DHFR and DHODH). These treatments are highly efficient but resistances that arose in South-East Asia complicate disease management and threaten elimination.[3] Most commonly used antimalarial medications are derived or inspired by natural products, such as quinine, artemisinin, atovaquone or doxycycline.[4] Natural products have been an incredible source of inspiration in drug discovery and fills a chemical space that is not reached by chemical synthesis.[5]

Here, we screened an in-house chemical library of hemisynthetic derivatives of the natural product trilobine (bisbenzylisoquinoline alkaloid) obtained from the plant *Cocculus hirsutus*. *C. hirsutus* is of the Menispermaceae family, is rich in alkaloids and a perennial climber widespread in tropical and sub-tropical regions. Various parts of this plant are notably used in Asia for the treatment of fevers.[6] Activity of the trilobine hemisynthetic library was tested against *P. falciparum* asexual blood stage parasites, the stage responsible for all clinical symptoms. Hits belonging to the natural product family showed killing activity in the nanomolar range against *P. falciparum*. Chemical modifications of the lead compound improved the activity against the disease-causing stage of malaria, but also in the stages that transmit the disease. This compound is fast-acting and has sustained activity in multi-drug-resistant clinical isolates originating from Cambodia, including artemisinin-resistant. Efforts were made to develop derivatives with an optimized *in vivo* efficacy in an experimental mouse malaria model and to decipher the protein target of these natural product derivatives.

RESULTS

Trilobine hemisynthetic derivatives are active against *P. falciparum* asexual blood stage

Screening of an in-house chemical library that targets distinct human epigenetic factors[7,8] identified hits against asexual blood stages of *P. falciparum*, belonging to the double bridge bisbenzylisoquinoline family of alkaloids found in *C. hirsutus*. We measured the activity of 94 natural and hemisynthetic derivatives. We fixed the threshold for activity at IC_{50} of 200 nM and identified compounds **31** and **84** (Figure 1A), the latter being the most active with a mean IC_{50} of 130 nM. This compound was then chosen as the lead compound. Hemi-synthesis of **84** from the trilobine natural analog cocsuline (**4**) is described in Figure 1B.

Compound 84 is a fast-acting compound and is active throughout the asexual blood cycle

Compound **84** was tested for its stage-specific activity in the asexual blood cycle (Figure 2A). Tightly synchronized *P. falciparum* (NF54) parasites were exposed to concentrations corresponding to 3x or 10x the IC_{50} of **84**. Parasites were treated for 6h windows covering the entire 48h cycle. Survival was assessed by counting parasites in a thin blood smear 72h post-invasion (hpi). Compound **84** is active throughout the entire asexual cell cycle, with the highest killing activity between 18 and 42hpi. Importantly, **84** is active in the early ring stage (0-6hpi), with less than 5% surviving parasites at 10x the IC_{50} and about 20% survival at 3x the IC_{50}. As 6h of incubation were sufficient to obtain efficient parasite killing, we assessed the speed of action of **84** using the Parasite Reduction Rate assay (PRR) developed by Sanz et al.[9] We found that **84** is acting as fast as dihydroartemisinin (DHA), the active metabolite of artemisinin derivatives (Figure 2B), and chloroquine, in comparison to the slow-acting compound pyrimethamine.

Compound 84 has a sustained activity in *P. falciparum* multi-drug resistant field isolates

Since compound **84** is active in early ring stages and is fast-acting, we assessed its activity against multi-drug resistant field isolates adapted to culture, notably isolates resistant to artemisinin (Figure 2C). Using IC_{50} as a proxy, **84** has a similar IC_{50} in the laboratory strain NF54 and drug-sensitive isolates originating from Cambodia (median of 147 nM). Interestingly, isolates resistant to artemisinin have an increased sensitivity to **84** (median IC_{50} of 88 nM) especially when they carry additional resistance to piperaquine and amodiaquine, with median IC_{50} values dropping to 46 and 36 nM respectively (Figure 2C, left panel). In the Ring-stage Survival Assay (RSA),[10] DHA shows, as expected, a difference in survival between artemisinin-susceptible and artemisinin-resistant isolates (DHA concentration used corresponds to 200 times the IC_{50}). Compound **84** shows no difference in survival, whichever the resistance background of the isolates, when used at a concentration of 3 times the IC_{50}. The observed survival values correspond to the value obtained in the laboratory line NF54 (Figure 2A). Notably, **84** combined with DHA reduces almost to zero the survival of artemisinin-resistant strains (Figure 2C, right), indicating a synergistic effect.

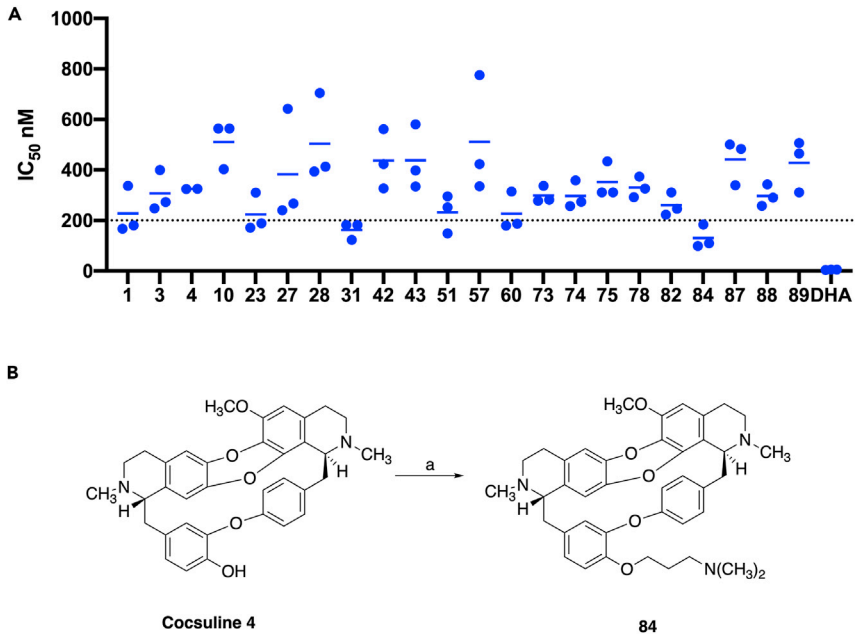

Figure 1. IC_{50} of the most potent bisbenzylisoquinolines out of the 94 derivatives of the chemical series and hemi-synthesis of compound 84

(A) IC_{50} was measured in triplicate using *P. falciparum* NF54 strain, in three independent experiments. Growth was determined using the SYBR Green I assay after 72h incubation with the compounds. Points represent individual IC_{50} value (in nM) measured in each experiment and lines represent the mean. Compound **84** is the most active with a mean IC_{50} of 130 nM and was selected as the lead compound. DHA = dihydroartemisinin.

(B) Hemi-synthesis of **84** starting from the natural compound cocsuline (**4**): a) *i*) NaH, DMF, 0°C then RT, 30 min; *ii*) 3-dimethylaminopropylchloride, KI, 80°C, 15h.

Preclinical studies reveal that 84 binds to human plasma proteins

To assess compound **84** *in vivo*, preclinical studies were realized to test the cytotoxicity, microsomal stability, and plasma binding properties. Microsomal stability half-life of **84** was higher than 60min and the cytotoxicity in HepG2 human cells resulted in a selectivity index superior to 75 (data not shown). However, **84** was found highly bound to plasma protein (>99% in both humans and mice), thus only a very minor fraction would be able to reach the target in the infected host cell. To overcome this problem, the chemical modulation of **84** was carried out (Figure 3A).

Chemical synthesis of novel derivatives and *in vitro* activity

Selective double demethylation of the two methoxy substituents of the natural product isotrilobine (**2**) was realized to obtain two phenol groups that were substituted with the corresponding alkylamines to afford compounds **125-129** (Figure 3A, Data S3 and Scheme S1 related to Figure 3A). Importantly, compound **125** showed significantly lower human plasma protein binding (90% in human plasma and 95% in mice) and a similar antimalarial activity (123 nM) as compound **84** (130 nM), a good microsomal stability (half-life >60min) and acceptable cytotoxicity. Moreover, the citrate salt of this compound is soluble in water since no aggregation was found by Dynamic Light Scattering at a concentration of 15 mM (Figure 3B).

Compound 125 increases survival *in vivo*

Thus compound **125** was chosen for *in vivo* studies. First, pharmacokinetic properties were assessed (Figure 3C): **125** has a long half-life (superior to 24h) with very slow elimination after a single dose administered either *i.v.*, *p.o.* or *i.p.*. Plasma concentration reached up to 600 ng/mL, 30min after *i.p.* injection. Antimalarial *in vivo* activity was then conducted using the Peter's 4-day suppressive test in C57BL/6 mice infected *i.v.* with *Plasmodium berghei* ANKA (Figure 3D). While the lowest dosage at 10 mg/kg *i.p.* increased the survival by 3.5 days compared to the control, it did not reduce parasitemia. Most interestingly, dosing at 20 mg/kg *i.p.* increased survival by 5 days and significantly lowered parasitemia compared

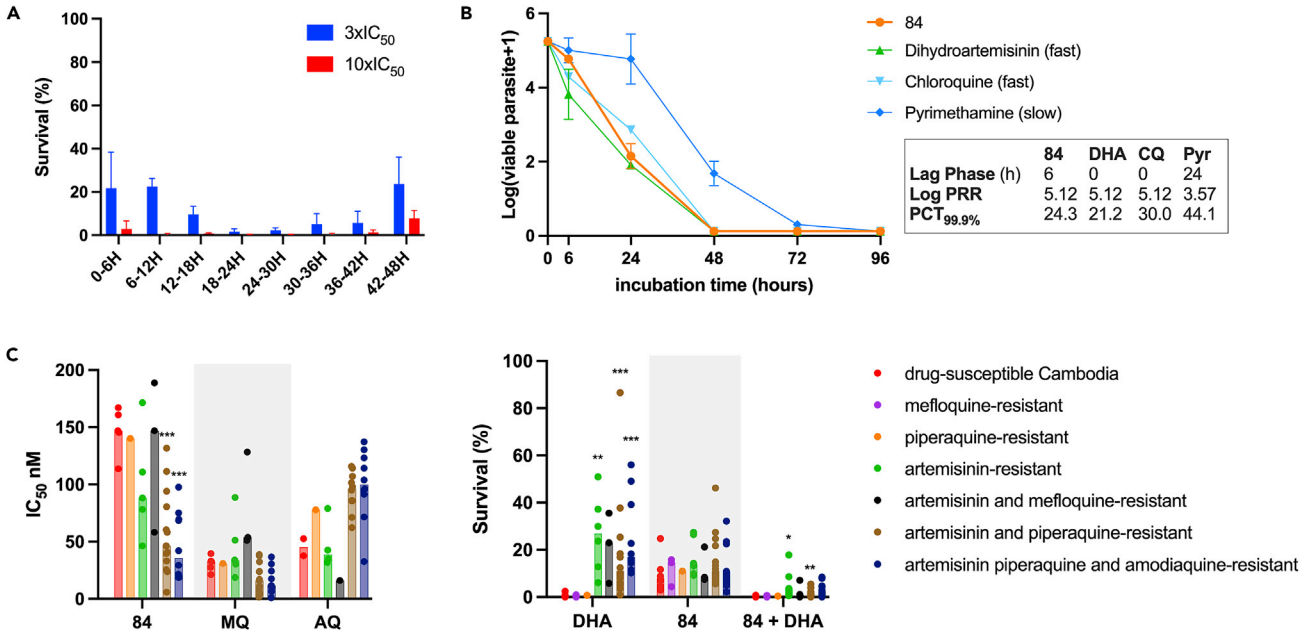

Figure 2. Activity of compound 84 in *P. falciparum* asexual blood stages

(A) Stage-specific activity in *P. falciparum* NF54 asexual cell cycle. Tightly synchronized parasites (0-3h post-invasion) were incubated with **84** for 6h, for 8 consecutive, 6h periods, covering the 48h cell cycle, at two different concentrations (3x and 10x the IC_{50}). Survival rate was evaluated 72h after synchronization (n = 3 independent experiments).

(B) *In vitro* parasite reduction rate (PRR). *P. falciparum* culture containing mostly ring and mono-infected red blood cells (RBC) were incubated with **84** or reference drugs (dihydroartemisinin (DHA), chloroquine (CQ) and pyrimethamine (Pyr)) for different time windows (6h, 24h, 48h, 72h, and 96h), washed, serially diluted in fresh RBC and allowed to grow for 3 weeks, then growth was assessed using the SYBR Green I assay.[9] N = 1 experiment run in duplicate.

(C) Activity against *P. falciparum* multi-drug resistant field isolates adapted to culture. Left graph: IC_{50}s (dots) of **84** and two reference drugs (mefloquine, MQ, and desethylamodiaquine, AQ) obtained against Cambodian field isolates are plotted versus the type of resistance carried by the isolate. Bars represent the median value. Right graph: Percentage of survival using the Ring-stage Survival Assay (RSA). Tightly synchronized ring-stage parasites (0-3h post-invasion) were incubated with 700 nM dihydroartemisinin (DHA), 3x the IC_{50} of **84** (equivalent to 400 nM), or the combination of both, for 6h. After the drugs are washed out and the parasites are allowed to grow until 72h post-synchronization. Parasite survival is assessed by counting parasitemia in 10,000 RBC in a thin blood smear, in comparison to a DMSO-treated control.[10] Bars represent the median value. Statistics = multiple Mann-Whitney tests in comparison with the drug-sensitive Cambodia condition (if discovery: ***p value < 0.001; **p value < 0.01; *p value < 0.05).

to the control group (two-way ANOVA with Dunett's correction, adjusted p value < 0.0001). However, complete cure was not achieved, and dose escalation was avoided due to potential toxicity in mice at higher doses.

125 is active in the transmission and liver stages

First, we tested compound **125** in early (stage IIb-III) and late (stage IV-V) gametocytes (Figure 4A). This compound has an IC_{50} of around 1 μM in both stages in *P. falciparum* NF54 gametocytes and was slightly more active in the Cambodian strain 3601E1 resistant to artemisinin (Kelch13 R539T) with an IC_{50} of 700 nM (Figure 4B). Interestingly, the IC_{50s} were identical in both early and late gametocyte developmental stages, while antimalarials are usually less efficient against stage V, which is in a temporary quiescent state. For example, puromycin, used here as a reference (Figure 4B), does not reach complete killing.

We then assessed the efficacy of parasite development in *Anopheles* mosquito stages by adding **125** to the infectious blood meal. The effect on parasite transmission was evaluated by counting the number of midgut oocysts, 10 days after the blood feeding (Figure 4C). Compound **125** significantly decreased the oocyst number at 10 μM without an increase in mosquito mortality compared to DMSO (data not shown).

Lastly, we tested compound **125** in primary human hepatocytes infected with *P. falciparum* sporozoites. Sporozoites invasion was performed for 3h, then cells were washed to remove remaining sporozoites and treated with **125** for 72h. Parasite survival was assessed by counting the number of intracellular parasite

A

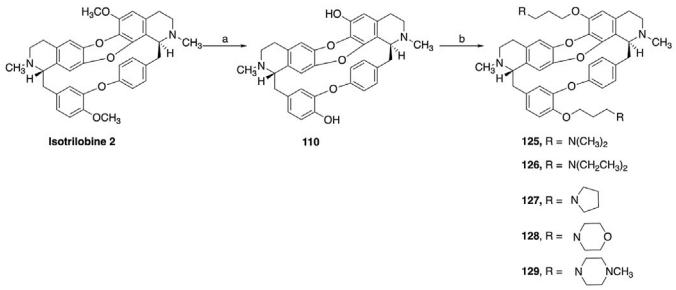

B

Compound ID	Pf IC_{50} (nM)	aggregation	Plasma binding (fraction bound, %)		microsomal stability (half-life, min)		Cytotoxicity (nM)
			mouse plasma	human plasma	mouse	human	HEPG2
84	130+/-35	No	99.8	99.6	> 60	> 60	>10,000
125	123+/-66	No	95.1	90.7	> 60	> 60	2,412
126	130+/-67	Yes	nd	nd	nd	nd	nd
127	136+/-69	No	98.7	97.1	> 60	> 60	504
128	170+/-44	Yes	99.8	99.5	25.0	16.1	521
129	148+/-48	Yes	99.6	98.0	> 60	> 60	365

C

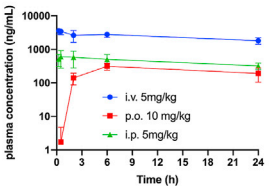

D

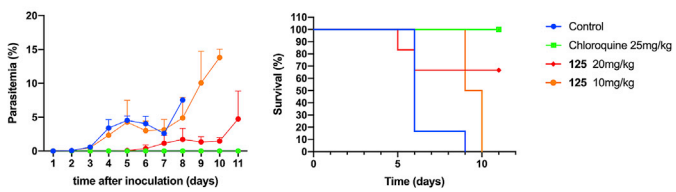

Figure 3. Compound 84 and its derivatives: toward the best candidate for *in vivo* studies

(A) General synthesis of compounds **125-129**. a) *i*) NaH, EtSH, DMF, 0°C, 30 min; *ii*) isotrilobine **2**, 150°C, 30 min; b) *i*) NaH, DMF, 0°C, 30 min; *ii*) desired chloro-derivative, 80°C, 1 ON, 25-45%.

(B) Table reporting the mean IC_{50} measured against *P. falciparum*, the solubility of the compound, the plasma binding fraction in mouse and human plasma, microsomal stability measured in mouse and human microsomes and the cytotoxicity measured in HepG2 human cell line, for **84** and its derivatives.

(C) Pharmacokinetic profile of compound **125** after a single dose of compound, administered either intravenously (*i.v.*, 5 mg/kg), *per os* (*p.o.*, 10 mg/kg) or intraperitoneally (*i.p.*, 5 mg/kg). Mean plasmatic concentration (+/−SD) is represented in ng/mL versus time (5 timepoints over 24h).

(D) *In vivo* activity of **125** in C57BL/6 mice infected with *P. berghei* ANKA. Mice were treated *i.p.*, 2h after parasite *i.v.* inoculation, for 4 days, with a daily regimen of 20 mg/kg or 10 mg/kg of **125** or 25 mg/kg of chloroquine or vehicle control. Parasitemia (mean ± SD) and survival were followed over 11 days.

forms using immunofluorescence staining with anti-HSP70 antibody. We observed a dose-dependent inhibition of parasite development in hepatocytes (Figure 4D), indicating that **125** targets proteins expressed during multiple life cycle stages of *P. falciparum*.

Investigation of *P. falciparum* cellular targets

To decipher the mode of action of this family of bisbenzylisoquinoline alkaloids, we synthesized a chemical probe **132** (Data S3 related to Figure 5A) derived from the parent natural product trilobine (compound **1**) and harboring a photo-activable benzophenone and a terminal alkyne group (Figure 5A). It was used to photo-crosslink directly in cells proteins bound to the probe or in its vicinity and, by 1,3-dipolar cycloaddition (CuAAC), to simultaneously label the cross-linked proteins with an azide derivative containing both a fluorescent reporter (TAMRA) and biotin for protein pull-down followed by mass spectrometry analysis and gel electrophoresis visualisation.[14] The probe **132** has a similar IC_{50} as trilobine (790 nM versus 410 nM, Figure S1 related to Figure 5), indicating that the derivatization was not impeding *in-cellulo* target engagement. It was then used to treat parasites either alone or in competition with increasing concentrations of the parent compound trilobine **1**. Harvested parasites were saponin-lysed to remove hemoglobin contaminants and then parasite pellets were resuspended and UV-irradiated at 365 nm to crosslink the compound with the nearby target. Cells were then lysed and the click reaction was initiated in parasite extracts. Purified functionalized proteins were then enriched using neutravidin beads, digested, and finally analyzed via LC−MS/MS (Figure 5A). In gel fluorescence of the different conditions is shown in Figure 5B. Target

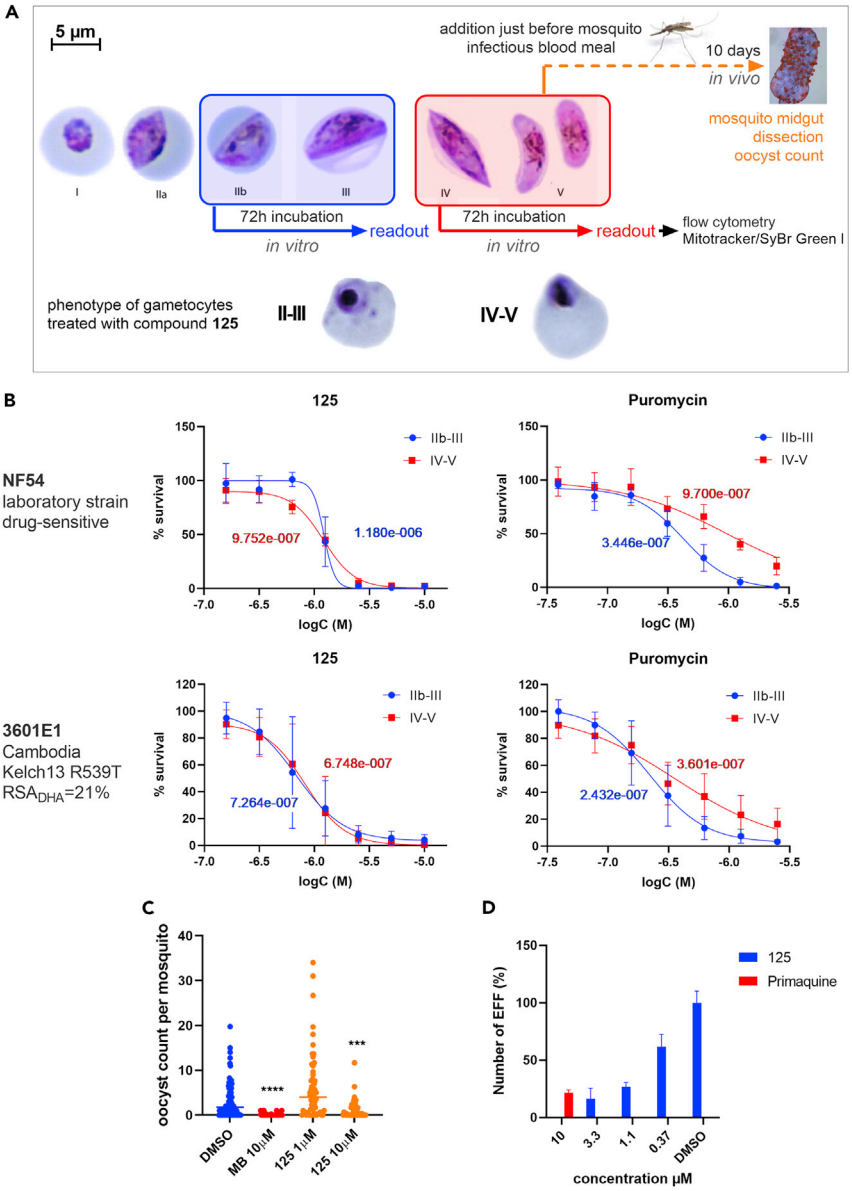

Figure 4. Activity of compound 125 in transmission and liver stages

(A) Scheme showing the methodology used to assess anti-transmission activity. Early (IIb-III, blue) and late (IV-V, red) stage gametocytes were treated *in vitro* for 72h before survival was assessed using a flow cytometry method (SyBR Green I and Mitotracker deep red FM dyes). Bottom images represent the phenotype of early and late-stage gametocytes treated with 5 µM of compound **125**. For *in vivo* mosquito studies (represented in orange), treatment was added to the infectious blood meal, containing mature stage V gametocytes, just before mosquito feeding. After 10 days of development, the number of oocysts was counted in each mosquito midgut. Pictures of gametocytes are taken and adapted from Josling and Llinás.[11]

(B) Gametocytocidal activity of **125** against early (IIb-III) and late (IV-V) stage gametocytes in NF54 drug-susceptible strain and 3601E1, a cloned Cambodian isolate bearing R539T Kelch13 mutation that confers 21% survival after exposure to 700 nM dihydroartemisinin (DHA) in the RSA. Puromycin was used as a positive control. N = 3 independent experiments run in triplicates (mean ± SD).

(C) Impact of compound **125** on parasite development in the mosquito. Each dot represents the number of oocysts counted in each mosquito midgut and the line represents the median. MB = methylene blue. N = 4 independent experiments. Statistical analysis was done using the Mann-Whitney test. ****p value < 0.0001; ***p value = 0.0002.

(D) Activity of **125** in *P. falciparum* liver stages (mean with SD). Compound was added after sporozoites invasion of human primary hepatocytes. Media containing an increasing concentration of the compound was changed daily for 72h. Primaquine at 10 µM was used as a positive control. Exoerythrocytic forms (EEF) survival was assessed using immunostaining of parasites with *Pf*HSP70 antibody. N = 1 experiment run in triplicate.

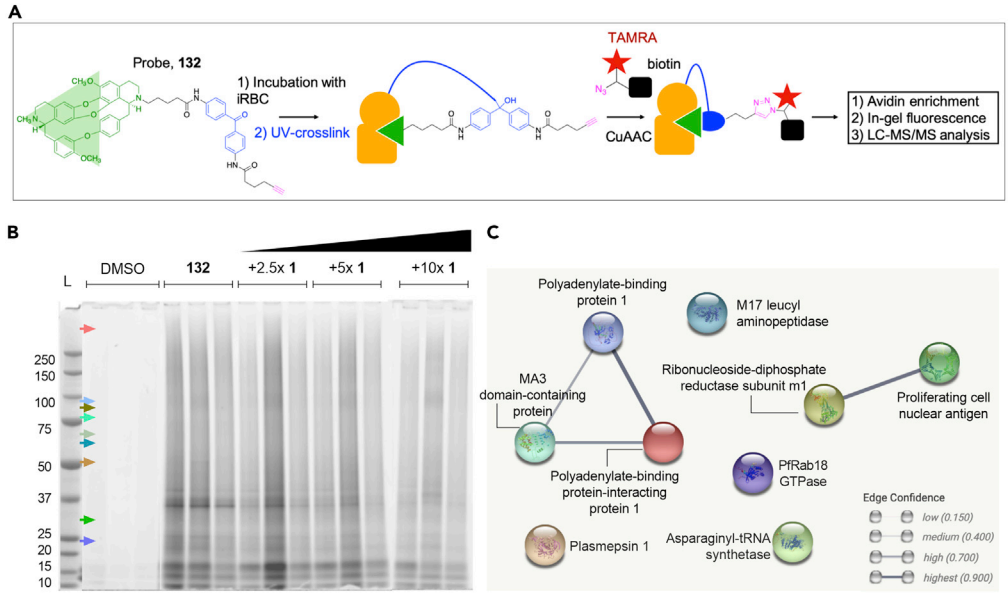

D

PlasmoDB code	Protein name	Essential?	MW	GO term biological process
PF3D7_0211800	asparagine--tRNA ligase	Y	70.5	tRNA aminoacylation for protein translation
PF3D7_0807300	ras-related protein Rab-18	Y	23.1	Intracellular protein transport, small GTPase mediated signal transduction
PF3D7_1107300	polyadenylate-binding protein-interacting protein 1, putative	N	381.9	MIF4G domain containing protein, translation initiation factor activity
PF3D7_1224300	polyadenylate-binding protein 1, putative	Y	97.2	RNA processing, Binds the poly(A) tail of mRNA
PF3D7_1361900	proliferating cell nuclear antigen 1	Y	30.6	Auxiliary protein of DNA polymerase delta, involved in the control of DNA replication by increasing the polymerase's processibility during elongation of the leading strand
PF3D7_1407900	plasmepsin I	+/-	51.5	Proteolysis, hemoglobin catabolic process
PF3D7_1437200	ribonucleoside-diphosphate reductase large subunit, putative	Y	96.9	Provides the precursors necessary for DNA synthesis. Catalyzes the biosynthesis of deoxyribonucleotides from the corresponding ribonucleotides
PF3D7_1446200	M17 leucyl aminopeptidase	Y	67.8	Proteolysis, metalloaminopeptidase
PF3D7_1457300	MA3 domain-containing protein, putative	Y	76.0	Negative regulation of transcription, DNA-templated; translation initiation factor binding

Figure 5. Chemical pull-down to decipher the protein targets

(A) Chemical pull-down strategy. Chemical probe **132**, containing a photo-activable crosslinker moiety (in blue) and a reactive alkyne (in pink) to initiate the bioorthogonal 1,3-cycloaddition reaction, is incubated with parasites. After photo-crosslinking, click-labeling with biotin and a fluorescent reporter (TAMRA), and avidin-biotin affinity purification, enriched protein partners were analyzed by mass spectrometry.

(B) In-gel fluorescence of the pulled-down proteins labeled with TAMRA. Probe **132** was incubated with parasites at a concentration of 10 μM and competition with trilobine (**1**) was done at 25 μM (2.5x), 50 μM (5x), and 100 μM (10x), in triplicate. DMSO was used as a negative control. Colored arrows indicate the molecular weight of the proteins with matched colors in panel C.

(C) Clustering of enriched protein selected for their (i) decreasing quantity in competition with trilobine, (ii) enrichment compared to DMSO, and (iii) consistency between triplicates. Clustering was realized using the STRING[12] database.

(D) Table reporting the essentiality,[13] molecular weight (MW) and GO term biological process of the chemical pull-down enriched proteins.

deconvolution was done by plotting the competition curves *i.e.* protein abundance when probe **132** was used alone (10 μM) or in competition with 25 μM, 50 μM or 100 μM of parent compound **1**. Only candidates producing curves with consistency between triplicates were selected. Among these, proteins that were not enriched compared to DMSO were discarded, as well as proteins with shared peptides (multigenic families). Clustering of the selected proteins was done using STRING software.[12] Two different pathways were revealed: polyadenylate-binding protein 1 complex (PABP1 and its partners), involved in protein translation, and proliferating cell nuclear antigen (PCNA1) involved in DNA replication and DNA methylation (Figures 5C and 5D). Noteworthy, none of those candidates has been previously associated with drug targeting by antimalarials or drug-resistance mechanisms.

DISCUSSION

We explored the activity of bisbenzylisoquinoline alkaloids, isolated from the plant *C. hirsutus*, in *P. falciparum*. The antimalarial activity of trilobine and its natural alkaloids analogs was significantly improved by synthesizing a chemical library of hemisynthetic compounds. Importantly, none of the

multi-drug resistant clinical isolates from Cambodia showed cross-resistance to the lead compounds, indicating that this chemical scaffold targets parasite pathways distinct from commonly used antimalarial drugs. Furthermore, lead compounds are fast-acting, comparable to chloroquine and artemisinin. Another important activity is that the lead molecule kills the early-ring stage, which is able to resist high concentration of artemisinin by entering into dormancy.[15] The lead compound **84** can restore antimalarial activity in artemisinin-resistant isolates when combined with DHA (Figure 2C), which highlights the potential of this chemical series to be used in combination with artemisinin. Natural bisbenzylisoquinoline alkaloids extracted from diverse plants have been already described for their antimalarial properties[16–22] and previous re-sensitization has been described for bisbenzylisoquinolines in chloroquine-resistant *P. falciparum* strains, as well as in tumor cells resistant to vinblastin.[20,23] Here we report the first hemisynthetic study resulting in compounds with improved pharmacological properties of these natural products, active in resistant strains including artemisinin-resistant ones and all along the life cycle of the parasite.

As compound **84** was found to be highly bound to plasma protein (>99%), precluding its use for *in vivo* studies, new derivatives were synthesized resulting in compound **125** with a decreased plasma protein binding. Compound **125** showed sustained antimalarial activity (123 nM), water solubility, high microsomal stability, and low cytotoxicity (Figure 3B). Pharmacokinetic studies revealed rapid absorption and very slow elimination with an elimination half-life far superior to 24h (Figure 3C). *In vivo* antimalarial activity in mice infected with *P. berghei* shows that four doses at 20 mg/kg of **125** delay the onset of parasitemia and increase mice survival by 5 days (Figure 3D).

Compound **125** is also targeting transmission stages (*in vitro* and *in vivo*) and liver stages of *P. falciparum*, though at higher concentration than in the blood stage (Figure 4). This indicates that the protein target(s) are expressed in different stages of *Plasmodium*'s life cycle. To decipher the targeted proteins, we synthesized a chemical probe from the parent compound trilobine and used UV-affinity capture and chemical pull-down followed by mass spectrometry analysis. Target deconvolution of mass spectrometry hits revealed different protein interactions with the probe. The predicted targets have in common to have house-keeping functions in diverse vital pathways of *P. falciparum* such as the polyadenylate binding protein 1 (PABP1, Pf3D7_1224300) and the proliferating cell nuclear antigen 1 (PCNA1, Pf3D7_1361900) (for details, see Figure 5D). PABP1, its protein partner polyadenylate binding protein interacting protein 1 (PABP-IP1, Pf3D7_1107300) and MA3 domain-containing protein (MDCP, Pf3D7_1457300) are involved in protein translation.[24,25] They bind to the polyA tail of mRNA and are part of a complex with Eukaryotic translation Initiation Factor 4F (EIF4F) to mediate the recruitment of ribosomes to mRNA.[26] The PCNA1 protein is involved in DNA replication and DNA methylation,[27] and in DNA-damage response.[28] PCNA1 is clustering with the ribonucleoside-diphosphate reductase subunit m1 (RNRm1, Pf3D7_1437200). This protein has an important role in DNA synthesis since it catalyzes the rate-limiting step of *de novo* synthesis of the deoxyribonucleotides by reducing the corresponding ribonucleotides.[29] To our knowledge, the identified pathways have never been targeted by antimalarials or have been involved in a malaria parasite drug-resistance mechanism. Indeed, we were not able to obtain resistant parasites upon low-concentration continuous treatment with the compounds (data not shown). Interestingly, these pathways are vital for the other life cycle stages targeted by the compounds (transmission, liver stages). These proteins are well conserved in other malaria species (*Plasmodium malariae, vivax, ovale, and knowlesi*), and thus likely to kill these species as well, except for PABP-IP1, which is non-essential and not annotated in the genomes of *Plasmodium vivax, ovale, and knowlesi*. We show here for the first time that the bisbenzylisoquinoline trilobine could affect specific proteins involved in DNA replication and protein translation. This work lays out strategies for further studies to validate the protein target(s) by complementary methods such as the use of recombinant proteins. Defining the target will help the future preclinical drug-development process, by facilitating the improvement of selectivity compared to human homologs protein(s) in order to optimize the compound and deliver a new drug candidate.

In conclusion, we identified a novel chemical scaffold derived from a natural product with activities against all life cycle stages that interacts with diverse essential parasite pathways.

Limitations of the study

The main limitation is due to the supply of plant extracts. Importantly, the plant is abundant, and all parts contain isotrilobine, which is easily separated and is the precursor of lead **125**. Additional studies are necessary to characterize the target and this will help optimize the best lead.

STAR★METHODS

Detailed methods are provided in the online version of this paper and include the following:

- KEY RESOURCES TABLE
- RESOURCE AVAILABILITY
  - Lead contact
  - Materials availability
  - Data and code availability
- EXPERIMENTAL MODEL AND SUBJECT DETAILS
  - HepG2 cells
  - Primary human hepatocytes
  - *P. falciparum* continuous culture
  - *In vivo* antimalarial activity
- METHOD DETAILS
  - Chemical library synthesis
  - Chemical synthesis
  - Compound solubility/aggregation
  - Microsomal stability and plasma binding
  - Cytotoxicity in HepG2 cells
  - Inhibition activity in the asexual stages
  - Stage-specificity during the asexual cell cycle
  - *In vitro* parasite reduction rate (PRR)
  - Activity against *P. falciparum* Cambodian field isolates
  - Pharmacokinetic studies
  - Activity against synchronous gametocytes
  - Standard membrane feeding assay
  - Liver-stage activity
  - UV-affinity capture and protein pull-down
  - Protein digestion
  - LC-MS/MS analysis
  - Protein identification and quantification
  - Pull-down data analysis
- QUANTIFICATION AND STATISTICAL ANALYSIS

SUPPLEMENTAL INFORMATION

Supplemental information can be found online at https://doi.org/10.1016/j.isci.2023.105940.

ACKNOWLEDGMENTS

We thank Bertrand Raynal of the Plateforme de Biophysique Moléculaire, in C2RT Pasteur Institute, for technical help. We thank the Center for Production and Infection of *Anopheles* (CEPIA) in Institut Pasteur for the mosquito breeding and handling. We thank Bruno Vitorge and Remy Lemeur from the Institut Pasteur Biological NMR Technological Plat-form for assisting with NMR experiments, Frédéric Bonhomme of the CNRS-Institut Pasteur UMR3523 Organic Chemistry Unit for performing HRMS analysis. This work was supported by Institut Pasteur-Institut Carnot (S-CR18089-02B15 DARRI CONSO INNOV 46-19; S-PI15006-10A INNOV 05-2019 ARIMONDO IARP 2019-PC), Pasteur Transversal Research Program (PTR 233-2019 HALBY), Pasteur Swiss Foundation grant, Agence Nationale de la Recherche (ANR-20-CE18-0006 EpiKillMal), Pasteur-Roux-Cantarini Fellowship and French Parasitology consortium ParaFrap, Grant (ANR-11-LABX0024).

AUTHOR CONTRIBUTIONS

The article was written through the contribution of all authors. Conceptualization, F.N., A.S., L. H., and P.B.A.; methodology, F.N., I.D., H.H., L.H., and P.B.A.; formal analysis, G.M.; investigation, F.N., I.D., H.H., F.R, S.T, L.M.S., A.T, C.J., V.C.D, S.G, A.L., M.M., M.D, L.H., and P.B.A.; Resources, B.W.; writing – original draft, F.N., I.D., A.S., and P.B.A; writing – review and editing, Y.M., N.M, D.P., C.L., F.S., M.M., G.M., B.W., and L.H.; visualization, F.N.; supervision, F.N., A.S., L.H., and P.B.A.; funding acquisition, F.N., A.S., L.H., and P.B.A. All authors have given approval to the final version of the article.

DECLARATION OF INTERESTS

Authors F.N., H.H., L.H., A.S. and P.B.A. declare a patent entitled Trilobine derivatives and use thereof in the treatment of malaria reference WO2021/224491 A1 (11/11/2021).

INCLUSION AND DIVERSITY

We support inclusive, diverse, and equitable conduct of research.

Received: November 23, 2022
Revised: December 23, 2022
Accepted: January 5, 2023
Published: February 17, 2023

REFERENCES

1. World Health Organization (2022). World Malaria Report 2022. https://www.who.int/teams/global-malaria-programme/reports/world-malaria-report-2022.

2. Wong, W., Bai, X.-C., Sleebs, B.E., Triglia, T., Brown, A., Thompson, J.K., Jackson, K.E., Hanssen, E., Marapana, D.S., Fernandez, I.S., et al. (2017). The antimalarial Mefloquine targets the Plasmodium falciparum 80S ribosome to inhibit protein synthesis. Nat. Microbiol. *2*, 17031. https://doi.org/10.1038/nmicrobiol.2017.31.

3. Menard, D., and Dondorp, A. (2017). Antimalarial drug resistance: a threat to malaria elimination. Cold Spring Harb. Perspect. Med. *7*, a025619. https://doi.org/10.1101/cshperspect.a025619.

4. Wells, T.N.C. (2011). Natural products as starting points for future anti-malarial therapies: going back to our roots? Malar. J. *10*, S3. https://doi.org/10.1186/1475-2875-10-S1-S3.

5. Guiguemde, W.A., Shelat, A.A., Garcia-Bustos, J.F., Diagana, T.T., Gamo, F.-J., and Guy, R.K. (2012). Global phenotypic screening for antimalarials. Chem. Biol. *19*, 116–129. https://doi.org/10.1016/j.chembiol.2012.01.004.

6. Logesh, R., Das, N., Adhikari-Devkota, A., and Devkota, H.P. (2020). Cocculus hirsutus (L.) W.Theob. (Menispermaceae): a review on traditional uses, phytochemistry and pharmacological activities. Medicines (Basel) *7*, 69. https://doi.org/10.3390/medicines7110069.

7. Halby, L., MENON, Y., Kaloun, E.B., Long, C., and Arimondo, P.B. (2017). Hemi-synthetic Trilobine Analogs for Use as a Drug.

8. Menon, Y., Long, C., Sautel, F., and Arimondo, P.B. (2017). Trilobine and its Natural Analogs for Use as a Drug.

9. Sanz, L.M., Crespo, B., De-Cózar, C., Ding, X.C., Llergo, J.L., Burrows, J.N., García-Bustos, J.F., and Gamo, F.-J. (2012). P. falciparum in vitro killing rates allow to discriminate between different antimalarial mode-of-action. PLoS One *7*, e30949. https://doi.org/10.1371/journal.pone.0030949.

10. Witkowski, B., Amaratunga, C., Khim, N., Sreng, S., Chim, P., Kim, S., Lim, P., Mao, S., Sopha, C., Sam, B., et al. (2013). Novel phenotypic assays for the detection of artemisinin-resistant Plasmodium falciparum malaria in Cambodia: in-vitro and ex-vivo drug-response studies. Lancet Infect. Dis. *13*, 1043–1049. https://doi.org/10.1016/S1473-3099(13)70252-4.

11. Josling, G.A., and Llinás, M. (2015). Sexual development in Plasmodium parasites: knowing when it's time to commit. Nat. Rev. Microbiol. *13*, 573–587. https://doi.org/10.1038/nrmicro3519.

12. Szklarczyk, D., Gable, A.L., Nastou, K.C., Lyon, D., Kirsch, R., Pyysalo, S., Doncheva, N.T., Legeay, M., Fang, T., Bork, P., et al. (2021). The STRING database in 2021: customizable protein-protein networks, and functional characterization of user-uploaded gene/measurement sets. Nucleic Acids Res. *49*, D605–D612. https://doi.org/10.1093/nar/gkaa1074.

13. Zhang, M., Wang, C., Otto, T.D., Oberstaller, J., Liao, X., Adapa, S.R., Udenze, K., Bronner, I.F., Casandra, D., Mayho, M., et al. (2018). Uncovering the essential genome of the human malaria parasite Plasmodium falciparum by saturation mutagenesis. Science *360*, eaap7847. https://doi.org/10.1126/science.aap7847.

14. Pechalrieu, D., Assemat, F., Halby, L., Marcellin, M., Yan, P., Chaoui, K., Sharma, S., Chiosis, G., Burlet-Schiltz, O., Arimondo, P.B., et al. (2020). Bisubstrate-type chemical probes identify GRP94 as a potential target of cytosine-containing adenosine analogs. ACS Chem. Biol. *15*, 952–961. https://doi.org/10.1021/acschembio.9b00965.

15. Wellems, T.E., Sá, J.M., Su, X.-Z., Connelly, S.V., and Ellis, A.C. (2020). "Artemisinin resistance": something new or old? Something of a misnomer? Trends Parasitol. *36*, 735–744. https://doi.org/10.1016/j.pt.2020.05.013.

16. Srivastava, A.K., Kumar, A., and Misra, N. (2016). Quantum chemical studies on cocsuline using density functional theory and its docking into dihydrofolate reductase receptor. Main Group Chem. *15*, 97–106. https://doi.org/10.3233/MGC-150187.

17. Otshudi, A.L., Apers, S., Pieters, L., Claeys, M., Pannecouque, C., De Clercq, E., Van Zeebroeck, A., Lauwers, S., Frédérich, M., and Foriers, A. (2005). Biologically active bisbenzylisoquinoline alkaloids from the root bark of Epinetrum villosum. J. Ethnopharmacol. *102*, 89–94. https://doi.org/10.1016/j.jep.2005.05.021.

18. Angerhofer, C.K., Guinaudeau, H., Wongpanich, V., Pezzuto, J.M., and Cordell, G.A. (1999). Antiplasmodial and cytotoxic activity of natural bisbenzylisoquinoline alkaloids. J. Nat. Prod. *62*, 59–66. https://doi.org/10.1021/np980144f.

19. Guinaudeau, H., Böhlke, M., Lin, L.-Z., Angerhofer, C.K., Cordell, G.A., and Ruangrungsi, N. (1997). (+)-Angchibangkine, a new type of bisbenzylisoquinoline alkaloid, and other dimers from pachygone dasycarpa. J. Nat. Prod. *60*, 258–260. https://doi.org/10.1021/np960568e.

20. Frappier, F., Jossang, A., Soudon, J., Calvo, F., Rasoanaivo, P., Ratsimamanga-Urverg, S., Saez, J., Schrevel, J., and Grellier, P. (1996). Bisbenzylisoquinolines as modulators of chloroquine resistance in Plasmodium falciparum and multidrug resistance in tumor cells. Antimicrob. Agents Chemother. *40*, 1476–1481. https://doi.org/10.1128/AAC.40.6.1476.

21. Marshall, S.J., Russell, P.F., Wright, C.W., Anderson, M.M., Phillipson, J.D., Kirby, G.C., Warhurst, D.C., and Schiff, P.L. (1994). In vitro antiplasmodial, antiamoebic, and cytotoxic activities of a series of bisbenzylisoquinoline alkaloids. Antimicrob. Agents Chemother. *38*, 96–103. https://doi.org/10.1128/AAC.38.1.96.

22. Likhitwitayawuid, K., Angerhofer, C.K., Cordell, G.A., Pezzuto, J.M., and Ruangrungsi, N. (1993). Cytotoxic and antimalarial bisbenzylisoquinoline alkaloids from Stephania erecta. J. Nat. Prod. *56*, 30–38. https://doi.org/10.1021/np50091a005.

23. Ye, Z.G., Van Dyke, K., and Castranova, V. (1989). The potentiating action of tetrandrine in combination with chloroquine or qinghaosu against chloroquine-sensitive and resistant falciparum malaria. Biochem. Biophys. Res. Commun. *165*, 758–765. https://doi.org/10.1016/s0006-291x(89)80031-2.

24. Tuteja, R. (2009). Identification and bioinformatics characterization of translation initiation complex eIF4F components and

poly(A)-binding protein from Plasmodium falciparum. Commun. Integr. Biol. *2*, 245–260. https://doi.org/10.4161/cib.2.3.8843.

25. Tuteja, R., and Pradhan, A. (2009). Isolation and functional characterization of eIF4F components and poly(A)-binding protein from Plasmodium falciparum. Parasitol. Int. *58*, 481–485. https://doi.org/10.1016/j.parint.2009.09.001.

26. Gingras, A.C., Raught, B., and Sonenberg, N. (1999). eIF4 initiation factors: effectors of mRNA recruitment to ribosomes and regulators of translation. Annu. Rev. Biochem. *68*, 913–963. https://doi.org/10.1146/annurev.biochem.68.1.913.

27. Vasuvat, J., Montree, A., Moonsom, S., Leartsakulpanich, U., Petmitr, S., Focher, F., Wright, G.E., and Chavalitshewinkoon-Petmitr, P. (2016). Biochemical and functional characterization of Plasmodium falciparum DNA polymerase δ. Malar. J. *15*, 116. https://doi.org/10.1186/s12936-016-1166-0.

28. Mitra, P., Banu, K., Deshmukh, A.S., Subbarao, N., and Dhar, S.K. (2015). Functional dissection of proliferating-cell nuclear antigens (1 and 2) in human malarial parasite Plasmodium falciparum: possible involvement in DNA replication and DNA damage response. Biochem. J. *470*, 115–129. https://doi.org/10.1042/BJ20150452.

29. Chakrabarti, D., Schuster, S.M., and Chakrabarti, R. (1993). Cloning and characterization of subunit genes of ribonucleotide reductase, a cell-cycle-regulated enzyme, from Plasmodium falciparum. Proc. Natl. Acad. Sci. USA *90*, 12020–12024. https://doi.org/10.1073/pnas.90.24.12020.

30. March, S., Ramanan, V., Trehan, K., Ng, S., Galstian, A., Gural, N., Scull, M.A., Shlomai, A., Mota, M.M., Fleming, H.E., et al. (2015). Micropatterned coculture of primary human hepatocytes and supportive cells for the study of hepatotropic pathogens. Nat. Protoc. *10*, 2027–2053. https://doi.org/10.1038/nprot.2015.128.

31. Trager, W., and Jensen, J.B. (1976). Human malaria parasites in continuous culture. Science *193*, 673–675.

32. Malmquist, N.A., Sundriyal, S., Caron, J., Chen, P., Witkowski, B., Menard, D., Suwanarusk, R., Renia, L., Nosten, F., Jiménez-Díaz, M.B., et al. (2015). Histone methyltransferase inhibitors are orally bioavailable, fast-acting molecules with activity against different species causing malaria in humans. Antimicrob. Agents Chemother. *59*, 950–959. https://doi.org/10.1128/AAC.04419-14.

33. Peters, W. (1975). The chemotherapy of rodent malaria, XXII. The value of drug-resistant strains of P. berghei in screening for blood schizontocidal activity. Ann. Trop. Med. Parasitol. *69*, 155–171.

34. Ishino, T., Orito, Y., Chinzei, Y., and Yuda, M. (2006). A calcium-dependent protein kinase regulates Plasmodium ookinete access to the midgut epithelial cell. Mol. Microbiol. *59*, 1175–1184. https://doi.org/10.1111/j.1365-2958.2005.05014.x.

35. Nardella, F., Halby, L., Hassan, H., Menard, D., Scherf, A., and Arimondo, P.B. (2021). Trilobine Derivatives and Their Use Thereof in the Treatment of Malaria.

36. Nardella, F., Halby, L., Hammam, E., Erdmann, D., Cadet-Daniel, V., Peronet, R., Ménard, D., Witkowski, B., Mecheri, S., Scherf, A., et al. (2020). DNA methylation bisubstrate inhibitors are fast-acting drugs active against artemisinin-resistant Plasmodium falciparum parasites. ACS Cent. Sci. *6*, 16–21. https://doi.org/10.1021/acscentsci.9b00874.

37. Duffy, S., Loganathan, S., Holleran, J.P., and Avery, V.M. (2016). Large-scale production of Plasmodium falciparum gametocytes for malaria drug discovery. Nat. Protoc. *11*, 976–992. https://doi.org/10.1038/nprot.2016.056.

38. Ponnudurai, T., Lensen, A.H., Leeuwenberg, A.D., and Meuwissen, J.H. (1982). Cultivation of fertile Plasmodium falciparum gametocytes in semi-automated systems. 1. Static cultures. Trans. R. Soc. Trop. Med. Hyg. *76*, 812–818. https://doi.org/10.1016/0035-9203(82)90116-x.

39. March, S., Ng, S., Velmurugan, S., Galstian, A., Shan, J., Logan, D.J., Carpenter, A.E., Thomas, D., Sim, B.K.L., Mota, M.M., et al. (2013). A microscale human liver Platform that supports the hepatic stages of Plasmodium falciparum and vivax. Cell Host Microbe *14*, 104–115. https://doi.org/10.1016/j.chom.2013.06.005.

40. Lubin, A.S., Rueda-Zubiaurre, A., Matthews, H., Baumann, H., Fisher, F.R., Morales-Sanfrutos, J., Hadavizadeh, K.S., Nardella, F., Tate, E.W., Baum, J., et al. (2018). Development of a photo-cross-linkable diaminoquinazoline inhibitor for target identification in Plasmodium falciparum. ACS Infect. Dis. *4*, 523–530. https://doi.org/10.1021/acsinfecdis.7b00228.

41. Cox, J., Neuhauser, N., Michalski, A., Scheltema, R.A., Olsen, J.V., and Mann, M. (2011). Andromeda: a peptide search engine integrated into the MaxQuant environment. J. Proteome Res. *10*, 1794–1805. https://doi.org/10.1021/pr101065j.

42. Cox, J., and Mann, M. (2008). MaxQuant enables high peptide identification rates, individualized p.p.b.-range mass accuracies and proteome-wide protein quantification. Nat. Biotechnol. *26*, 1367–1372. https://doi.org/10.1038/nbt.1511.

43. Ritz, C., Baty, F., Streibig, J.C., and Gerhard, D. (2015). Dose-response analysis using R. PLoS One *10*, e0146021. https://doi.org/10.1371/journal.pone.0146021.

STAR★METHODS

KEY RESOURCES TABLE

REAGENT or RESOURCE	SOURCE	IDENTIFIER
Antibodies		
PfHSP70	StressMarq Biosciences	Cat# SPC-186, RRID:AB_1608355)
Deposited data		
Proteome data	PRIDE repository	Proteomics Identifications (PRIDE) (RRID:SCR_003411)
Experimental models: Cell lines		
HEPG2 cell line	ATCC	RRID:CVCL_0027
3T3-J2	IZSLER	Cat# BS CL 153, RRID:CVCL_W667
Experimental models: Organisms/strains		
C57BL/6 mice	MGI	Cat# 2159769, RRID:MGI:2159769

RESOURCE AVAILABILITY

Lead contact

Further information and requests for resources and reagents should be directed to and will be fulfilled by the lead contact, Paola B. Arimondo (paola.arimondo@pasteur.fr).

Materials availability

There are restrictions to the availability of compounds due to necessity to resynthesise them *ad hoc*.

Data and code availability

Data. The mass spectrometry proteomics data have been deposited to the ProteomeXchange Consortium via the PRIDE partner repository with the dataset identifier PXD036288.

Project Webpage:http://www.ebi.ac.uk/pride/archive/projects/PXD036288.

FTP Download:ftp://ftp.pride.ebi.ac.uk/pride/data/archive/2023/01/PXD036288.

Code. This paper does not report original code.

Additional information. Any additional information required to reanalyse the data reported in this paper is available from the lead contact upon request.

EXPERIMENTAL MODEL AND SUBJECT DETAILS

HepG2 cells

Human HepG2 (hepatocellular carcinoma, RRID:CVCL_0027) were grown according to the provider instructions and at 37°C and 5% CO_2.

Primary human hepatocytes

Cryopreserved primary human hepatocytes (purchased from BioIVT) were co-cultured with J2-3T3 murine embryonic fibroblasts (gift of Howard Green, Harvard Medical School) as described previously.[30] Cultures were maintained in Dulbecco's Modified Eagle Medium (DMEM, Corning) with 10% fetal bovine serum (GIBCO), 1% ITS (insulin/transferrin/selenous acid and linoleic acid, BD Biosciences), 7 ng/mL glucagon (Sigma-Aldrich), 40 ng/mL dexamethasone (Sigma-Aldrich), 15 mM HEPES (GIBCO), and 100 mg/mL penicillin-streptomycin (Corning). Cells were kept at 37°C in a 5% CO_2 environment.

P. falciparum continuous culture

P. falciparum parasites were cultured using a standard protocol.[31] The laboratory strains used were NF54 and 3D7; that were grown in RPMI1640 supplemented with HEPES (25 mM) and L-glutamine (2 mM) (Gibco), 0.5% (m/v) Albumax I, hypoxanthine (100 nM) and gentamycin (16 ng/mL), at 37°C, under reduced oxygen pressure (5% O_2, 5% CO_2). *P. falciparum* clinical isolates used in this study were collected in the framework of the therapeutic efficacy surveillance program in Cambodia between 2017 and 2019. Culture was performed in the same condition as for laboratory strains except that 5% (v/v) human serum and 0.25% (m/v) Albumax II were used for serum supplementation.

In vivo antimalarial activity

All animal experiments performed in the manuscript were conducted in compliance with French animal welfare laws and Institut Pasteur Animal Care and Use Committee guidelines. *In vivo* activity was determined as previously described[32] following the Peters 4-day suppressive test[33] with slight modifications. 6-weeks old C57BL/6 female mice (Janvier Labs, MGI Cat# 2159769,RRID:MGI:2159769) were infected intravenously (*i.v.*) with 10^5 iRBC of *P. berghei* ANKA GFP-expressing parasites.[34] 2h post-infection, mice were randomly assigned to experimental groups and treated intraperitoneally (*i.p.*) for 4 days with **125** following a daily regimen of 20 mg/kg or 10 mg/kg, or 25 mg/kg of chloroquine, or the equivalent vehicle control. Parasitemia was quantified from blood samples collected every day by flow cytometry of 200,000 RBCs and confirmed by Giemsa-stained thin blood smears. The experiment was performed once (n = 6 mice per group).

METHOD DETAILS

Chemical library synthesis

Purification of trilobine and its natural products and hemi-synthesis of the trilobine derivatives are described in.[7,35]

Chemical synthesis

All chemicals were from Sigma-Aldrich, Alfa Aesar and FluoChem. NMR experiments were recorded on an Agilent DirectDrive 500 spectrometer (Agilent Technologies, Santa Clara) with a proton resonating frequency of 500 MHz. Spectra were recorded using VnmrJ 4.2A (Agilent Technologies). Chemical shifts are given in ppm. Coupling constants *J* are measured in Hz. Splitting patterns are designed as follows: s, singlet; bs broad singlet; d, doublet; bd broad doublet; t, triplet; brt, broad triplet; dd, doublet of a doublet; m, multiplet; ddd, doublet of a doublet of a doublet; q, quartet; p, quintet, sext, sextet. HRMS analysis were performed on a Q Exactive mass Spectrometer (Thermofisher) using direct injection. Samples were previously dissolved in a mix of water and acetonitrile (50/50) and 0.1% of formic acid. Full scans (150–2000 Da) were acquired in positive ion mode with a resolution of 70,000. The purity of all final compounds was verified to be higher than 95% using reversed-phase HPLC system (Agilent 1200 series) equipped with a diode-array detector on a C18 reverse phase column (Kromasil, 5 μm, 100 Å; 4.6 × 150 mm) at a flow rate of 1 mL min^{-1} with a linear gradient of acetonitrile in 10 mM triethylammonium acetate buffer over 20 min (05–95% CH_3CN).

Synthesis and chemical analysis of compounds **84, 125, 126, 127, 128** and **129** is detailed in the Data S1 and Data S2. The chemical synthesis of probe **132** is reported in Data S3.

Compound solubility/aggregation

Compounds were mixed with citrate (1:1) to obtain the salt and then diluted in water at a final concentration of 15 mM 20 μL of each sample was then screened for aggregates by Dynamic Light Scattering on a DnyaPro plate reader III (Wyatt technology).

Microsomal stability and plasma binding

Rat and human microsomal stability and plasma binding studies were outsourced at Fidelta Ltd., Zagreb, Croatia.

Cytotoxicity in HepG2 cells

Cytotoxicity was evaluated after 72h of drug treatment in 96-well plates by ATPlite (PerkinElmer) according to the manufacturer's protocol. Experiments were run in technical triplicates and at least in two biological replicates. GraphPad Prism 8 was used to interpolate IC_{50}. DMSO was used as control.

Inhibition activity in the asexual stages

IC_{50} values were obtained using a range of 7-point and 2-step serial dilutions starting at 2 μM, 0.7% starting parasitemia and 2% final hematocrit. Growth was assessed after 72h using the SYBR Green I assay. GraphPad Prism 8 was used to interpolate IC_{50} from three independent experiments run in triplicate. DHA and DMSO were used as positive and negative controls, respectively.

Stage-specificity during the asexual cell cycle

Stage-specificity was assessed using previously described methods.[36] Briefly, asexual NF54 parasites were tightly synchronized (0–3hpi) and incubated for 6h with compound **84** at 3× and 10× IC_{50} value, at 0, 6, 12, 18, 24, 30, 36, or 42hpi. Following each treatment, cells were pelleted, washed with 10 mL of RPMI medium, and put back into culture in a new plate. Parasitemia was assessed at 72h post-synchronization using Giemsa-stained thin blood smears. The percentage of survival was compared to DMSO-treated parasites. Data were obtained from three independent experiments (one well per condition).

In vitro parasite reduction rate (PRR)

The *in vitro* parasite reduction rate was adapted from Sanz et al.[9] 10^6 infected RBC containing mostly rings were cultivated separately with 10× the IC_{50} of **84** or reference drugs (DHA, Chloroquine (CQ) or Pyrimethamine (Pyr)) for 6h, 24h, 48h, 72h and 96h (0.5% starting parasitemia, 2% hematocrit of *P. falciparum* 3D7). After each incubation time, cells were washed and serially diluted (1/3) with fresh RBC. Growth was assessed after 3 weeks, using the SYBR green I assay. The number of wells showing parasite growth is correlated with the number of viable parasites at the different time points (as defined by Sanz et al.) and allows defining the growth parameters reported in Figure 2B. The experiment was performed once in duplicate.

Activity against *P. falciparum* Cambodian field isolates

P. falciparum isolates used in this study were collected in the framework of the therapeutic efficacy surveillance program in Cambodia between 2017 and 2019. PSA, RSA, AQSA and genotyping data have been performed in the Pasteur Institute in Cambodia. Parasites were chosen based on the pattern of multi-drug resistance they carry. IC_{50} values were obtained as previously described[36] with slight modifications: ring-synchronized cultures (2% hematocrit, 1% starting parasitemia) were incubated for 96h before growth measurement using the SYBR green I assay. A range of 11-point and 2-step serial dilutions, starting at 1 μM were used to assess the activity of **84**. Mefloquine (MQ) and monodesethylamodiaquine (dAQ) were used as positive controls. Experiments were performed in triplicate, with one biological replicate per isolate. Statistical analysis was performed using multiple Mann-Whitney tests in comparison with the *drug-sensitive Cambodia* condition.

Ring-stage survival assay (RSA)

The RSA[10] was determined by treating 0-3h synchronized ring-stage parasites, for 6h, with either DMSO, 700 nM DHA, 3xIC_{50} of **84** or the combination of both. The IC_{50} used was the one obtained against the NF54 strain. After 6h, drugs were washed out and parasites were put back into culture. Parasitemia was assessed at 72h post-synchronization using Giemsa-stained thin blood smears. Percentage of survival was compared to DMSO-treated parasites and data were obtained from one independent experiment, in the different isolates. Statistical analysis was performed using multiple Mann-Whitney tests in comparison with the *drug-sensitive Cambodia* condition.

Pharmacokinetic studies

PK studies were outsourced at Fidelta Ltd., Zagreb, Croatia, according to standard procedures.

Activity against synchronous gametocytes

For this experiment, we used two different strains that retain their capacity to produce gametocytes: the drug-susceptible laboratory strain NF54 and an artemisinin-resistant (Kelch13 R539T) cloned Cambodian

isolate 3601E1. Synchronous gametocytes were induced following previously described methods[37] with slight modifications: trophozoite purification steps were performed using gelatin flotation (Plasmion). Media containing 0.05% (w/v) Albumax I was used until induction (day 0, corresponding to gametocyte-committed ring stage parasites), followed by a media containing 5% (v/v) human serum and 0.025% (w/v) Albumax I. Asexual parasite populations was removed by *N*-acetylglucosamine treatment for 5 days. Parasites were treated with **125** and the positive control puromycin to evaluate efficacy against early (day 4, stage IIb-III) and late-stage gametocytes (day 9, stage IV-V). Parasites, at approximately 1% starting gametocytemia, were seeded in 96-well plates at 2% final hematocrit and treated for 72h with a 7-point and 2-step serial dilutions of compounds starting at 10 μM for **125** or 2.5 μM for puromycin. Readout of parasite survival was done by flow cytometry (Guava 6HT, Luminex corp) using a Mitotracker Deep Red^{FM} (molecular probes, 50 μg, reference M22426) and SYBR™ Green I (10,000x concentrate in DMSO, Lonza) staining. SYBR Green I was used at a final dilution of 0.5x and Mitotracker at a final concentration of 100 nM, in prewarmed PBS (37°C). Data were acquired on 10,000 red blood cells, in triplicate, in 3 independent experiments.

Standard membrane feeding assay

The culture of gametocytes is performed in a semi-automated system developed in Nijmegen, Netherlands[38] at an initial parasitemia of 0.5%. After 4–6 days, the parasitemia reaches approximately 5–10% and gametocytogenesis is induced. The cultures are checked twice a week to evaluate the presence of the different stages of gametocyte development. Infectious stage V gametocytes are observed after approximately two weeks of culture. To assess the maturity of the male gametocytes, an aliquot of the culture is taken and the number of exflagellation events are counted under optical microscope, using a 400x magnification, by diluting infected red blood cells in human serum. Cultures containing mature gametocytes are diluted to 1:6 in a mix of 50% fresh red blood cells and 50% human serum. Compound **125** (1 or 10 μM final concentration), methylene blue (MB) (10 μM) or DMSO are added to this mix and fed to 50 *Anopheles stephensi* females per condition, using a membrane feeder. The mosquitoes are maintained at 26°C and 70% humidity with 10% sucrose as food source. Ten days post-infection, the mosquito midguts are dissected and stained with 0.25% fluorescein and the number of oocysts per midgut are counted. The results have been obtained in 4 independent experiments. Statistical analysis was done using Mann-Whitney test.

Liver-stage activity

Micropatterned human primary hepatocytes surrounded by supportive 3T3-J2 stromal cells (IZSLER Cat# BS CL 153, RRID:CVCL_W667)[39] were seeded on glass-bottom 96-well plates and infected the following day with 70,000 sporozoites per well of *P. falciparum* NF54. Cells were centrifuged at 700g for 5min to settle down the parasites. Sporozoites were allowed to invade for 3h before washing the cells, then fresh media containing drugs was added and changed daily. Cells were incubated for 72 h at 37°C and 5% CO_2 before fixation and permeabilization with ice-cold methanol and staining with dapi and PfHSP70 antibody (StressMarq Biosciences Cat# SPC-186, RRID:AB_1608355). Readout was done by counting PfHSP70-stained exoerythrocytic forms (EEF) in fluorescence microscopy. **125** was tested at 4 different concentrations, ranging from 10 to 0.37 μM, using a 3-fold dilution. Primaquine diphosphate at 10 μM was used as a control. Experiment was done once in triplicate.

UV-affinity capture and protein pull-down

Asynchronous *P. falciparum* NF54 cultures (1.10^8 parasites per condition) were treated for 1h with 10 μM of probe or DMSO. After 30min, the competitor was added in increasing concentration (DMSO, 25 μM, 50 μM or 100 μM of trilobine, **1**) for 30min before infected red blood cells (iRBC) were harvested, saponin-lysed in ice (0.15% saponin in PBS) and washed thoroughly in ice-cold PBS to remove hemoglobin contaminants. Parasite pellets were resuspended in PBS and irradiated for 1h at 365 nm, on ice, to crosslink the probe to its protein targets. Parasites were centrifuged and pellets were lysed in a buffer containing 1% SDS, 1 mM dithiothreitol (DTT) and protease inhibitors (Roche) in PBS. Protein concentration was determined and extracts were diluted to a concentration of 1 mg/mL. Click-labelling was done following described protocol[40]: 100 μL of extracts were treated with a 6 μL premix solution containing the following reagents to obtain a final concentration of: 60 μM of TAMRA-biotin-azide (Jena Bioscience, catalog number CLK-1048-5), 1 mM $CuSO_4$ in water (freshly prepared), 1 mM tris(2-carboxyethyl)phosphine (TCEP) and 100 μM tris[(1-benzyl-1*H*-1,2,3-triazol-4-yl)methyl]amine (TBTA). Tubes were shaken at room temperature for 1h after which proteins were precipitated with sequential addition and vortexing of methanol (200 μL), chloroform (50 μL) and ddH_2O (100 μL). Tubes were then centrifuged for 2 min at 14,000g and

the protein layer was washed twice with 200 μL of methanol. Methanol was discarded and remaining solvent was let to evaporate at room temperature. Proteins were resuspended in SDS buffer (1% SDS, 10 mM DTT). Samples were then enriched on avidin-coupled agarose beads (PierceNeutrAvidin Agarose, ThermoFisher Scientific; 50 μL, pre-washed three times in 0.2% SDS in PBS) by incubation with gentle shaking for 2h at room temperature to bind and enrich biotin-labeled proteins thanks to the probe. The supernatant was then removed, and the beads were washed with 1% SDS in PBS (3 × 500 μL), 4M urea in 50 mM ammonium bicarbonate (AMBIC) (2 × 300 μL) and 50 mM AMBIC (5 × 300 μL). This experiment was done in three independent replicates.

Protein digestion

Reduction of disulfide bonds of enrich biotin-labeled proteins in 50 mM AMBIC was achieved by addition of DTT to final concentration of 5 mM and incubation for 30 min at 56°C with shaking. Then, iodoacetamide (IAA) was added at a final concentration of 20 mM for cysteine alkylation, and samples were incubated in dark for 30 min at 37°C. Samples were digested for 4h using LysC (Promega, MA, USA). Subsequently, 1 μg of trypsin (Promega, MA, USA) was added, and samples were digested overnight at 37°C. Digestion was quenched by addition of formic acid (FA). The digest was subsequently desalted using Sep-Pak C18 cartridges (Waters) and lyophilized in vacuum for further analysis.

LC-MS/MS analysis

All the samples were analyzed on a Q Exactive Plus Hybrid Quadrupole-Orbitrap Mass Spectrometer coupled with an Easy nLC 1200 ultra-high pressure liquid chromatography system (Thermo Fisher Scientific) with solvent A of 0.1% formic acid and solvent B of 0.1% formic acid/80% acetonitrile. 1 μg of each sample was injected on a 75-μm ID PicoFrit column packed *in-house* to approximately 30-cm length with ReproSil-Pur C18-AQ 1.9-μm beads (Dr. Maisch). Column equilibration and peptide loading were done at 900 bars in buffer A (0.1% FA). Samples were separated at a 250 nL/min flow rate with a gradient of 2–7% buffer B in 5min, 23% buffer B in 70min, 23 to 45% buffer B in 30min, 45 to 95% buffer B in 5min, followed by a hold at 95% for 7min and back to 2% for 15min. Column temperature was set to 60°C. Mass spectrometer was operated in data-dependent acquisition mode. The MS instrument parameters were set as follows: MS1, r = 70,000; MS2, r = 17,500; MS1 AGC target of 3e6; MS2 for the 10 most abundant ions using an AGC target of 1e6 and maximum injection time of 60ms; and a 45s dynamic exclusion. The isolation window was set to 1.6m/z and normalized collision energy fixed to 28 for HCD fragmentation. Unassigned precursor ion charge states as well as 1, 7, 8 and >8 charged states were rejected and peptide match was disable.

Protein identification and quantification

Acquired LC-MS/MS raw data were analyzed using MaxQuant 1.5.3.8 version[41] using the Andromeda search engine[42] against *P. falciparum*, strain NF54 proteome database (5,548 entries, download from PlasmoDB) and human reference proteome (89,260 entries, download Jan2018), concatenated with usual known mass spectrometry contaminants and reversed sequences of all entries. All searches were performed with oxidation of methionine and protein N-terminal acetylation as variable modifications and cysteine carbamidomethylation as fixed modification. Trypsin was selected as protease allowing for up to two missed cleavages. The minimum peptide length was set to 7 amino acids. The false discovery rate (FDR) for peptide and protein identification was set to 0.01. The main search peptide tolerance was set to 4.5ppm and to 20ppm for the MS/MS match tolerance. One unique peptide to the protein group was required for the protein identification. The match between run was selected. A false discovery rate cut-off of 1% was applied at the peptide and protein levels. All mass spectrometry proteomics data have been deposited at ProteomeXchange Consortium via the PRIDE partner repository with the dataset identifier PXD036288 (RRID:SCR_003411).

Pull-down data analysis

MaxQuant LFQ values were filtered for contaminants and the dose-response curves of all proteins with a triplicate >0 LFQ value for the DMSO-dosed pulldown were fitted using a four-parameter log-logistic regression using an R script that utilizes the 'drc' package.[43] Manual inspection of the curves helped select the potential targets which were set in a functional context using STRING.[12]

QUANTIFICATION AND STATISTICAL ANALYSIS

Statistical analysis used is reported in each relevant section of the methodology and in the corresponding figure legend.